

Molecular dynamics and electronic spectrum of C₆₀ crystals at high pressure

K. P. Meletov

Institute of Solid State Physics, Russian Academy of Sciences, Chernogolovka, Moscow Region, 142432 Russia

G. Kourouklis, D. Christofilos, and S. Ves

Aristotle University of Thessaloniki, Thessaloniki, GR-54006, Greece

(Submitted 12 May 1995)

Zh. Éksp. Teor. Fiz. **108**, 1456–1468 (October 1995)

The Raman scattering, luminescence, and absorption spectra of C₆₀ single crystals at $T=300$ K and pressures up to 15 GPa were measured. The pressure dependence of the frequencies of the Raman-active intramolecular optical phonons were determined and it was shown that phase transitions associated with orientational ordering of the molecules in a cubic lattice of fullerite occur at pressures of 0.4 and 2.4 GPa. The pressure shifts $\partial\omega_i/\partial P$ and the Grüneisen parameters $\gamma_i = -(\partial\omega_i/\omega_i)/(\partial V/V)$ of the intramolecular phonon modes in the orientationally ordered phase were determined. The magnitudes of the pressure shifts $\partial E/\partial P$ of the luminescence and absorption spectra were measured. The deformation potential $D = \partial E_g/\partial \ln(V_0/V)$ determined from these data is equal to 1.3 ± 0.1 eV. © 1995 American Institute of Physics.

1. INTRODUCTION

High-pressure experiments have played an important role in the investigations of the physical properties of fullerite since the development of an efficient method for producing this new material in macroscopic quantities.¹ These materials are of interest because of their unique structure and the extremely high theoretical hardness of the C₆₀ molecule, which exceeds that of diamond.² X-Ray diffraction measurements at high pressure have made it possible to determine the compressibility, the bulk moduli, and the equation of state of the C₆₀ crystal.^{3,4} The characteristic features of the diffraction pattern of the cubic structure of fullerite at high pressure, which are determined by the molecular form factor of C₆₀, indicate that the C₆₀ molecule is virtually incompressible up to pressures of 20 GPa.⁴ A great deal of effort has been expended on the investigation of the energy spectrum of C₆₀ at high pressure, the determination of the pressure shift of the absorption edge, and the pressure dependence of the band gap.^{5–9} Investigations of fullerite at very high pressures, where the distance between the nearest carbon atoms of neighboring molecules is comparable to the bond length within the molecule, are aimed at studying the stability of the molecule and chemical transformations occurring in the condensed state. The results obtained in this direction at pressures above 20 GPa are very contradictory. This can be judged from the reports of the fullerite–diamond,¹⁰ fullerite–amorphous carbon,^{5,9} and fullerite–“collapsed” fullerite⁷ phase transformations at high pressure.

Investigations of the phonon spectrum of C₆₀ by the method of Raman scattering have been used repeatedly for the purpose of identifying phase transitions and chemical transformations of the molecule at high pressure. The main results in this field are associated with the study of the stability of the molecule at pressures above 20 GPa^{5,7,9,10} as

well as orientational-ordering phase transitions in the initial pressure range.^{11,12} At the same time, investigations of molecular dynamics and electronic energy spectrum of C₆₀ at high pressure can yield important information about intermolecular interactions. Such information is necessary in order to improve the quality of the calculations of the band structure and phonon spectrum of C₆₀. Such numerical calculations agree fairly well with the normal-pressure experimental data, but the results of high-pressure numerical calculations performed thus far must be compared in detail with the measurements.^{13–15}

In the present paper the results of measurements of the absorption, luminescence, and Raman-scattering spectra of C₆₀ single crystals at high pressure are reported, the pressure dependence of the parameters of the electronic and phonon spectra is determined, and the results are compared with existing experimental and theoretical data. The pressure dependence of the frequencies of a number of intermolecular optical phonons is determined on the basis of the Raman-scattering data, and it is shown that the pressure shift of the phonon frequencies is linear in the entire pressure range. The magnitude of the shift changes abruptly at phase transitions, associated with the orientational ordering of the molecules in the cubic lattice of C₆₀, at pressures of 0.4 and 2.4 GPa. The pressure shifts of the long-wavelength edge of the absorption spectrum and the short-wavelength edge of the luminescence spectrum are determined from the absorption and luminescence spectra, and the results fall within the limits of error of the measurements. The Grüneisen parameters of the intramolecular phonon modes in the orientationally ordered phase and the magnitude of the deformation potential ($D = 1.3 \pm 0.1$ eV) are determined. The results obtained are compared with theoretical calculations of the band structure of C₆₀.

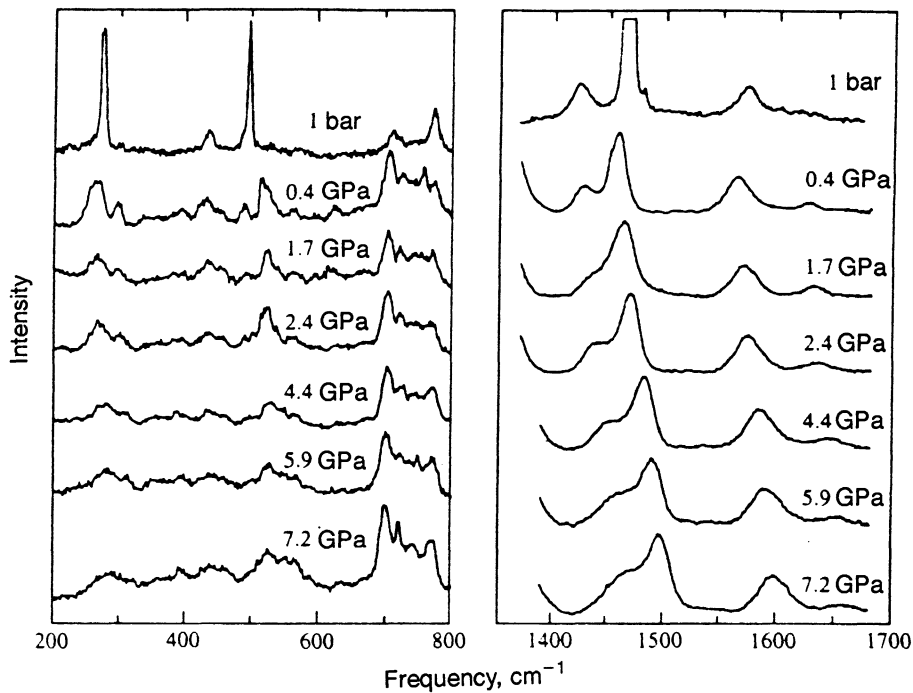


FIG. 1. Raman-scattering spectra of C_{60} crystals at $T = 300$ K and different pressures.

2. EXPERIMENT

Single crystals of fullerite C_{60} were grown from material prepared by the method of Ref. 1. According to mass-spectrometric data, the material was at least 99% pure. The absorption spectra were measured on thin C_{60} single crystals with transverse dimensions of $100 \times 100 \mu\text{m}^2$ and characteristic thicknesses of $1\text{--}5 \mu\text{m}$. Well-faceted crystals with a mirror-smooth surface and with characteristic dimensions of $100 \times 50 \times 20 \mu\text{m}^3$ were selected for the measurements of the Raman-scattering and luminescence spectra. Mao–Bell and Merrill–Bassett type diamond-anvil cells were used for the measurements at high pressures.¹⁶ The experimental sample was placed in a hole of diameter $150 \mu\text{m}$ in a $100 \mu\text{m}$ thick stainless steel gasket after compression. A 4:1 mixture of methanol and ethanol alcohols was used as the pressure-transmitting medium. The pressure was measured to within ~ 0.1 GPa according to the shift of the R_1 luminescence line of ruby.¹⁷ The Raman-scattering spectra were measured on a DILOR XY-500 triple monochromator with a liquid-nitrogen cooled multichannel optical linear array. The luminescence spectra were measured on a Spex double monochromator, equipped with a photon-counting system and a cooled photomultiplier with a GaAs photocathode. The 514.5 nm line of an argon laser was used to excite the luminescence and Raman scattering in the backscattering geometry. The laser beam power was less than 10 mW immediately in front of the chamber, and the diameter of the excitation spot was $\sim 50 \mu\text{m}$. The spectra were measured in unpolarized light and a $\lambda/4$ plate was used to depolarize the laser radiation. The absorption spectra were measured on a MDR-23 monochromator by the method described previously in Ref. 6. All experimental results were obtained in multiple series of measurements with increasing and decreasing pressure.

3. RESULTS AND DISCUSSION

3.1. Phonon spectrum

The Raman-scattering spectra of C_{60} single crystals at room temperature and at pressures of up to 7.2 GPa for the frequency ranges 200–800 and 1400–1700 cm^{-1} are displayed in Fig. 1. The strong vibration of the diamond crystal lies in the intermediate frequency range. This makes it impossible to perform measurements of the much weaker phonon modes of C_{60} which fall into this range. The vibrational spectrum of a free C_{60} molecule contains 46 modes with the symmetry

$$\Gamma = 2A_g + 3F_{1g} + 4F_{2g} + 6G_g + 8H_g + A_u + 4F_{1u} + 5F_{2u} + 6G_u + 7H_u, \quad (1)$$

and taking degeneracy into account the total number of modes is equal to 174.¹⁸ The Raman-active modes are two A_g and eight H_g modes. In the crystal containing four molecules per unit cell the total number of modes is higher: 714 taking into account degeneracy. At the same time, because the crystal field lowers the symmetry, the degenerate modes can split and additional bands can appear in the Raman-scattering spectrum.^{19,20} $T = 300$ K, ten bands with frequencies ranging from 273 up to 1575 cm^{-1} are observed in the Raman-scattering spectrum of the films and crystals of C_{60} . These bands correspond to intramolecular phonon modes, whose frequencies are equal to the vibrational frequencies of C_{60} molecules in solutions.^{19,21} When the temperature decreases below the point of the orientational phase transition, bands with frequencies ranging from 50 to 100 cm^{-1} , corresponding to the intermolecular crystal phonons,²⁰ appear in the spectrum.

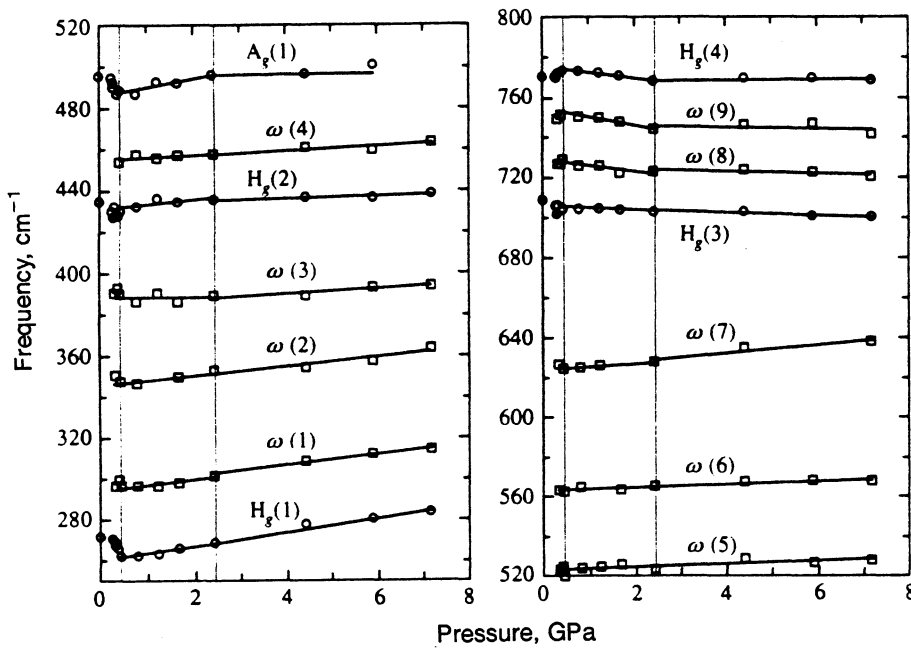


FIG. 2. Pressure shift of the frequency of the intramolecular phonons in the region 200–800 cm^{-1} .

The normal-pressure spectrum displayed in Fig. 1 contains eight of the ten intramolecular modes of C_{60} . The frequencies of these modes are presented in Table I and, to within the limits of error in the measurements, are equal to the previously obtained results.^{19,21} The strongest bands in the spectrum are due to the completely symmetric vibrations: The $A_g(1)$ breathing mode corresponds to in-phase stretch-compression of five- and six-member benzene rings and the $A_g(2)$ mode corresponds to antiphase stretch-compression. As one can see from Fig. 1, the Raman-scattering spectra change in a quite unusual manner as the pressure increases. At first, the phonon spectrum becomes softer and the pressure shift of most phonon modes is negative at pressures $P \leq 0.4$ GPa. As the pressure increases further, the character of the pressure dependence changes and virtually all phonon modes, with the exception of $H_g(3)$ and $H_g(4)$, become harder. It should also be noted that at $P = 0.4$ GPa additional modes appear in the Raman-scattering spectrum and all initial bands become appreciably weaker. A gradual change in the intensity of the close modes $H_g(7)$ and $A_g(2)$ is observed at pressures $P \geq 2.4$ GPa: The total intensity of the stronger mode $A_g(2)$ decreases and that of the weaker mode $H_g(7)$ increases.

The pressure dependence of the phonon frequencies of all intramolecular modes observed in the Raman-scattering spectrum is displayed in Figs. 2 and 3. The open circles represent the data for the main A_g and H_g modes and the open rectangles represent the $\omega(1) - \omega(9)$ modes newly appearing in the spectrum at pressures $P \geq 0.4$. These data were obtained with increasing pressure and the filled circles represent data for decreasing pressure. The results for increasing and decreasing pressure are identical to within the errors in the measurements and all observed effects are reversible with respect to the pressure. The solid straight lines are linear fits to the experimental data. The vertical lines correspond to pressures of 0.4 and 2.4 GPa, at which the pressure dependence of the phonon frequencies exhibits structure. The first

feature is associated with the change in the character of the pressure dependence of the phonon frequencies $\omega(P)$ at $P = 0.4$ GPa. The slope $d\omega/dP$ of the pressure dependence of the phonon frequencies for the modes $H_g(1)$, $H_g(2)$, $H_g(3)$, $H_g(8)$, $A_g(1)$, and $A_g(2)$ is negative at pressures $P \leq 0.4$ GPa and the phonon frequencies decrease as the pressure increases. For the phonon modes $A_g(4)$ and $H_g(7)$ we have $d\omega/dP > 0$ in this pressure range. As the pressure increases further to $P \geq 0.4$ GPa, $d\omega/dP$ changes sign and the frequencies of the phonon modes $H_g(1)$, $H_g(2)$, $H_g(8)$, $A_g(1)$, and $A_g(2)$ increase while the frequency of the mode $H_g(4)$ decreases. Note that for the mode $H_g(3)$ only $d\omega/dP$

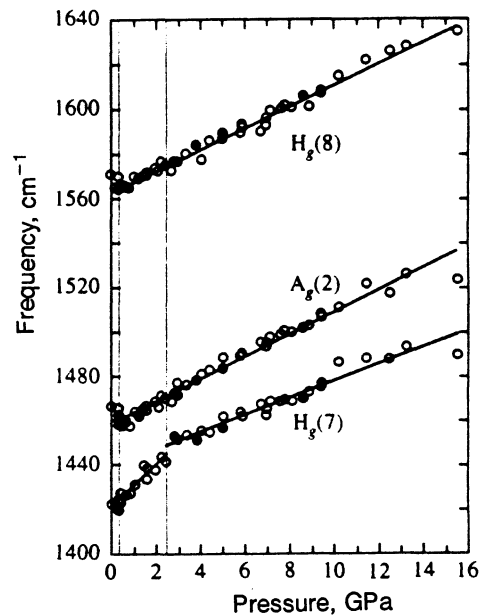


FIG. 3. Pressure shift of the frequency of intramolecular phonons in the region 1400–1640 cm^{-1} .

changes at $P=0.4$ GPa and this mode, like the mode $H_g(4)$, becomes softer in the entire range of measurements for $P \geq 0.4$ GPa. As far as the mode $H_g(7)$ is concerned, no appreciable changes in the pressure dependence of its frequency are observed at $P=0.4$ GPa. The second feature at $P=2.4$ GPa is due to the sharp change in the slope of the pressure dependence of the phonon frequencies for the modes $H_g(2)$, $H_g(3)$, $H_g(4)$, $H_g(7)$, $A_g(1)$, $\omega(3)$, $\omega(8)$, and $\omega(9)$. This change is most pronounced for the $H_g(7)$ mode, for which the slope $d\omega/dP$ decreases by more than a factor of 2 (see Table I). The phonon frequencies were determined by fitting a Lorentzian curve to the band contours; for the close phonon modes $H_g(7)$ and $A_g(2)$, it was also necessary to separate the band contours. As one can see from Fig. 3, the pressure dependence of these two modes at pressures in the range $0.4 \leq P \leq 2.4$ GPa suggests that they should cross at pressure $P \approx 9$ GPa. The sharp change in the slope of the pressure dependence of the $H_g(7)$ mode, the change in the crossing behavior of these modes to anticrossing, and the redistribution of their total intensities could indicate that these modes interact at pressures $P \geq 2.4$ GPa.

As noted previously,^{11,12} the features appearing in the pressure dependence of the phonon frequencies at 0.4 and 2.4 GPa could be associated with orientational-ordering phase transitions.^{22–25} The change in the sign of the pressure dependence of the phonon frequencies and the appearance of new bands in the Raman scattering spectrum at 0.4 GPa are associated with an orientational-ordering phase transition from a face-centered cubic (fcc) structure into a simple cubic (s.c.) structure.^{11,12} At normal pressure this transition occurs at $T=250$ K, and its temperature increases with pressure at a rate of approximately 10.6 K/kbar. This means that at room temperature it should occur at $P \approx 0.4$ GPa.^{22,23} As shown in recent work, the features at $P=2.4$ GPa could be due to the final stage of the orientational-ordering phase transition, associated with complete freezeout of jumps of C_{60} molecules between two equilibrium orientational positions in the s.c. structure.^{12,25} At normal pressure this transition occurs at $T \approx 85$ K,²⁴ and the pressure shift, determined according to our data assuming a linear pressure dependence, of the transition temperature is equal to ~ 9.2 K/kbar.

The changes occurring in the Raman-scattering spectrum at the phase transition could be associated with the change of symmetry of the vibrational modes of C_{60} in the crystalline phase, studied in detail in Ref. 18. The phonon modes of the free molecule, which correspond to the A_g and H_g representations of the icosahedral symmetry group I_h , correspond in the fcc structure to the representations T_h^3 of the symmetry group and change to $A_g \rightarrow A_g$ and $H_g \rightarrow E_g + F_g$ with partial removal of degeneracy.¹⁸ As a result of the orientational-ordering phase transition, their symmetry changes further and the degeneracy is removed, and in the s.c. structure they transform according to the representations of the group T_h^6 : $A_g \rightarrow A_g + F_g$ and $H_g \rightarrow A_g + 2 E_g + 5 F_g$.¹⁸ The low-temperature Raman-scattering spectra of C_{60} crystals, corresponding to the orientationally ordered phase contain additional bands, since all g -modes should be active in the s.c. structure.^{18,19} The appearance of the additional bands in the Raman scattering spectrum at pressures $P \geq 0.4$ GPa is also

apparently related to this. In this connection, it should be noted that the Raman-scattering spectrum of the orientationally disordered phase contains only bands which correspond to the main H_g and A_g intramolecular modes of the free molecule, and it is identical to the spectrum of C_{60} solutions.^{19–21} The absence of additional intramolecular modes in the spectrum of this phase is associated, in our opinion, with the fact that this phase cannot be regarded as a structure with translational symmetry in the full sense of this term. For the orientationally disordered phase, this is possible only in the case of a uniform distribution of charge in the C_{60} molecule. In reality, the real charge distribution is nonuniform because the charge density is different in the double and single carbon-carbon bonds. The change of the crossing to anticrossing behavior of the modes $H_g(7)$ and $A_g(2)$ could also be due to the change in symmetry of the crystal after the final stage of the orientational-ordering phase transition at $P=2.4$ GPa. Indeed, after the phase transition these modes split and they contain components of the same symmetry F_g and A_g , and their interaction can lead to repulsion of the modes and a redistribution of the intensity from the stronger into the weaker band.¹² It should be noted that the removal of degeneracy and splitting of bands are manifested in the high-pressure experimental spectra mainly in the broadening of the bands, since the splitting is small and is less than the half-width of the components.

All experimental data for the phonon spectrum of C_{60} are systematized in Table I. The normal-pressure phonon frequencies (for the modes $\omega(1) - \omega(9)$ at 0.4 GPa), the coefficients of the pressure shift $\partial\omega_i/\partial P$ for the regions $0.4 \leq P \leq 2.4$ and $P \geq 2.4$ GPa, and the values of the Grüneisen parameters $\gamma_i = -(\partial\omega_i/\omega_i)/(\partial V/V) = (B_0/\omega_i^0) \times (\partial\omega_i/\partial P)$ for all observed phonon modes are presented in the left-hand columns of Table I. The previously obtained experimental data for the normal-pressure phonon frequencies^{19,21} and the coefficients of the pressure shift⁵ are presented in the right-hand columns of Table I. A comparative analysis of the data given in the table shows that the normal-pressure phonon frequencies obtained in the present work are virtually identical to those of Refs. 19 and 21, while the results for the pressure shift are substantially different. This pertains primarily to the features which we discovered at pressures of 0.4 and 2.4 GPa in the pressure dependence of the phonon frequencies. It is important to note that not only are the values of the pressure coefficients different but there is also a qualitative difference in the pressure range $P \leq 0.4$ GPa, where, according to our data, virtually all phonon modes become softer. As far as the softening of the modes $H_g(3)$ and $H_g(4)$ in the entire pressure range is concerned, it was also observed in Ref. 5. The reliability of the experimental data on the softening of separate intramolecular modes has been confirmed in independent measurements of the infrared-absorption spectra of C_{60} .^{26,27} It is interesting to compare these results with the numerical calculations performed in Ref. 15 of the phonon spectrum of C_{60} under the hydrostatic compression conditions. The calculation for the orientationally ordered phase predicts only a positive pressure shift, which can reach $8.8 \text{ cm}^{-1}/\text{GPa}$ for separate intramolecular modes. It predicts splitting of some modes and

TABLE I.

Mode	Symmetry	ω_i^0 , cm ⁻¹	$\partial\omega_i/\partial P$, cm ⁻¹ /GPa		γ_i	ω_i^0 , cm ⁻¹	ω_i^0 , cm ⁻¹	$\partial\omega_i/\partial P$, cm ⁻¹ /GPa
			0.4 ≤ P ≤ 2.4	2.4 ≤ P				
H _g (1)	H _g	272	3.2	3.3	0.23	272	273	1.1
ω(1)		294	2.5	2.6	0.15			
ω(2)		345	2.9	2.9	0.15			
ω(3)		389	-0.2	1.1	-0.01			
H _g (2)	H _g	435	2.4	0.5	0.1	432	437	2.4
ω(4)		454	1.4	1.4	0.06			
A _g (1)	A _g	495	4.2	0.6	0.16	494	496	0.9
ω(5)		522	1.0	1.0	0.04	526		-0.5
ω(6)		563	0.8	0.7	0.03			
ω(7)		624	1.5	2.1	0.04			
H _g (3)	H _g	710	-0.8	-0.8	-0.02	708	710	-0.6
ω(8)		729	-2.9	-0.5	-0.07	724		
ω(9)		755	-4.1	-0.4	-0.1	759		
H _g (4)	H _g	772	-2.7	0.1	-0.06	772	774	-0.5
H _g (7)	H _g	1422	9.8	3.9	0.12	1422	1428	2.4
A _g (2)	A _g	1467	5.5	5.5	0.07	1463	1470	1.7
H _g (8)	H _g	1570	4.8	4.8	0.06	1566	1575	3.7

an increase in the dispersion of the phonon bands with increasing pressure, especially noticeable for intermolecular phonons, but it does not predict any features in the pressure dependence of the phonon frequencies. In this connection, the negative pressure shift of the modes H_g(3) and H_g(4) and the softening of the intramolecular modes in the orientationally disordered phase must also be explained. No reasons have been suggested for the negative pressure shift of the intramolecular phonon modes. As regards the softening of the modes in the orientationally disordered phase, we believe that it can be associated with the charge redistribution as a result of the orientational-ordering phase transition. The C₆₀ molecules in the orientationally ordered phase are oriented so that the double carbon-carbon bonds of the molecule with the higher electronic density are oriented toward the centers of the five- and six-member benzene rings of the nearest-neighbor molecules with a lower electronic density. This could produce some stretching of the bonds and softening of the intramolecular vibrations. Here it should be noted that the irreversible softening of the intramolecular mode A_g(2) in the Raman-scattering spectra observed by P. Eklund *et al.*,²⁸ is of a different nature and is associated with the photodimerization of C₆₀ under intense irradiation with light.

3.2. Electronic spectrum

The photoluminescence spectra of C₆₀ single crystals at room temperature and pressures up to 3 GPa are presented in Fig. 4. The spectrum at the lowest experimental pressure P=0.4 GPa (curve a) starts in the region 1.78 eV, where the fundamental absorption edge of C₆₀ also lies.⁶ The main maximum in the spectrum corresponds to an energy of ~1.62 eV, and the sharp peak near 1.78 eV is due to the luminescence of ruby and is employed to determine the pressure.¹⁷ The drop, marked by the arrow near 1.4 eV, in the red region of the spectrum is associated with the limit of the spectral sensitivity of the photomultiplier. The shape, position of the short-wavelength edge, and the main maximum of

the spectrum are close to those obtained in Ref. 29 for C₆₀ films at T=20 K. The curves b, c, d, and e correspond to spectra obtained at pressures of 1.0, 1.5, 2.4, and 2.7 GPa, respectively. As the pressure increases, the spectrum shifts in

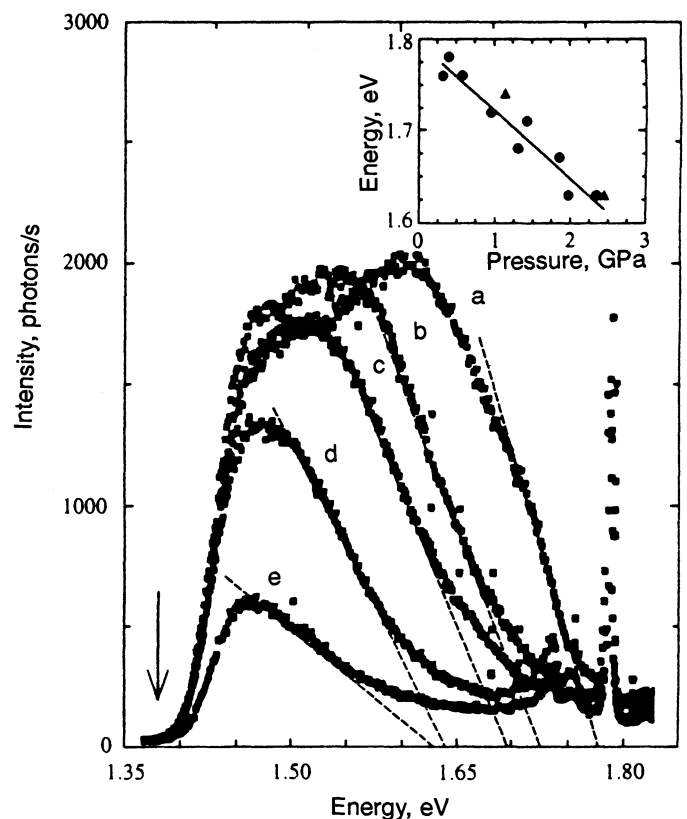


FIG. 4. Luminescence spectra of C₆₀ crystals at T=300 K and different pressures: a—0.4 GPa, b—1.0 GPa, c—1.5 GPa, d—2.2 GPa, and e—2.9 GPa. Inset: Pressure shift of the luminescence spectrum: points—increasing pressure, triangles — decreasing pressure.

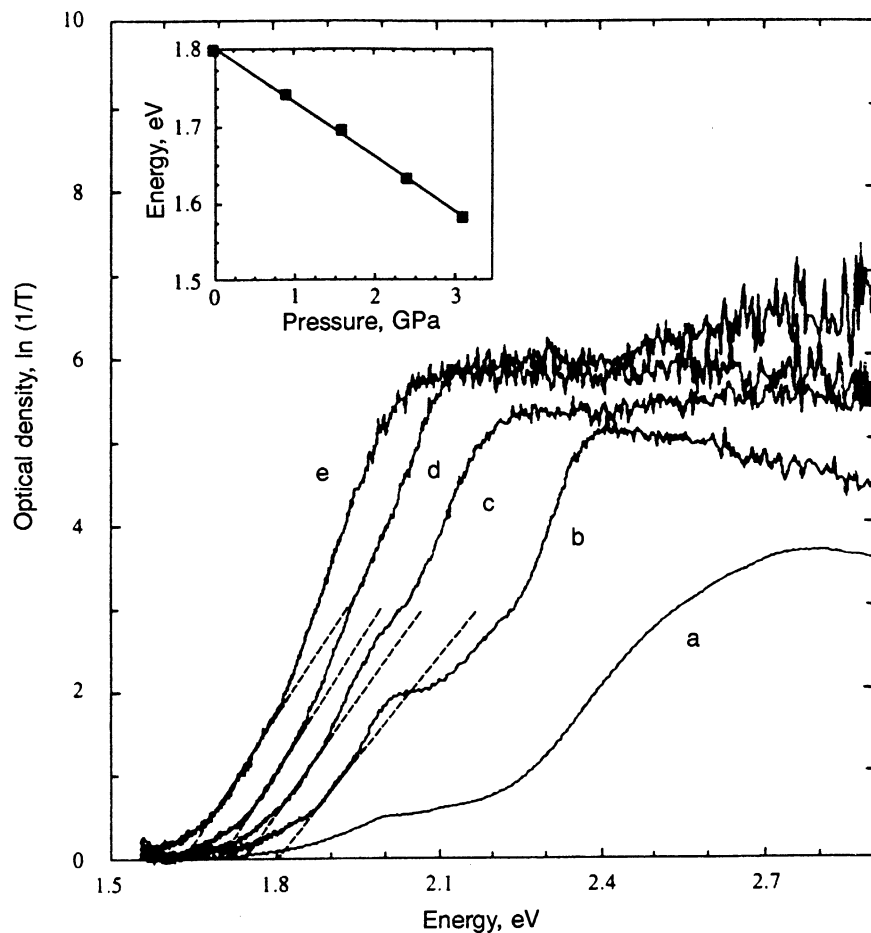


FIG. 5. Absorption spectra of C_{60} crystals at $T=300$ K and different pressures: a—thickness of $0.7 \mu\text{m}$ and $P=0.0001$ GPa; b, c, d, and e—thickness of $2.8 \mu\text{m}$ and pressures of 0.0001 , 0.9 , 1.6 , and 2.4 GPa, respectively. Inset: Pressure shift of the absorption edge.

the red direction and at 3 GPa most of the spectrum remains within the region of spectral sensitivity of the photomultiplier. It should be noted that the spectral sensitivity of the GaAs photocathode is virtually constant at energies above 1.45 eV, so that the shape of the spectrum in this region is the true shape and no corrections for the sensitivity of the photocathode are required. The dashed lines in the figure intersect the energy axis at energies that correspond approximately to the position of the short-wavelength edge of the luminescence spectrum. The pressure dependence, determined in this manner, of the position of the short-wavelength edge of the luminescence spectrum is displayed in the inset in Fig. 4. The small circles correspond to the measurements performed with increasing pressure and the triangles correspond to measurements performed with decreasing pressure. The solid straight line represents a fit of a linear function to the experimental data. The pressure shift dE/dP , determined from the luminescence spectrum, is equal to -0.074 ± 0.015 eV/GPa. It should be noted that the absolute magnitude of the shift is approximately two times smaller than that of the pressure shift $dE/dP = -0.138$ eV/GPa obtained in Ref. 8 from measurements of the photoluminescence spectra at pressures up to 3.2 GPa.

The spectral dependence of the optical density of C_{60} single crystals near the fundamental absorption edge at room temperature and different pressures are presented in Fig. 5. Curve (a) corresponds to the absorption spectrum of a crystal of thickness $\sim 0.7 \mu\text{m}$ thick crystal at normal pressure.

When a correction for thickness is made, it agrees in detail with the results of other work.^{7,29} Curve (b) corresponds to the absorption spectrum of a crystal of thickness $\sim 2.8 \mu\text{m}$ at the pressure with which saturation of optical density in the region of stronger absorption is associated. Curves (c), (d), and (e) correspond to the optical density of a crystal of thickness $2.8 \mu\text{m}$ at pressures of 0.9, 1.6, and 2.4 GPa, respectively. As the pressure increases, the spectrum shifts in the red direction and its shape changes somewhat. The step near 2 eV rapidly narrows with increasing pressure, and the step vanishes completely at $P \geq 2.5$ GPa. This means that the pressure shift in the region of stronger absorption, lying at higher energies, is larger than in the region adjoining the fundamental absorption edge. Incidentally, the possibility that the optical density in the region of stronger absorption increases with increasing pressure, which makes the stronger pressure shift visible, cannot be excluded. This feature in the pressure dependence of the absorption spectrum, which we discovered in Ref. 6 and which was confirmed in independent measurements,⁷ does not have an unequivocal explanation and requires further experimental study. The dashed straight lines in the figure intersect the energy axis at energies that correspond approximately to the long-wavelength absorption edge. At normal pressure the long-wavelength absorption edge lies at 1.8 eV and it coincides, to within the error of the measurements, with the position of the short-wavelength edge of the luminescence spectrum. The pressure dependence of the fundamental absorption edge determined

in this manner is displayed in the inset in Fig. 5 (filled triangles), and the solid straight line represents a linear fit to the experimental data. The pressure shift of the fundamental absorption edge is equal to -0.071 ± 0.01 eV/GPa and equals the pressure shift of the luminescence spectrum within the limits of error of the measurements.

The analysis of the pressure dependence of the parameters of the electronic spectrum is of interest from the standpoint of comparing the experimental data with the results of theoretical calculations of the energy spectra of the C_{60} molecule and the band structure of the C_{60} crystal. The system of π -electronic levels of the isolated molecule and their symmetry and degeneracy were determined in the first calculations of the spectrum of the free molecule performed by the Hückel method. It was determined that the highest filled electronic orbital corresponds to the h_u representation and the lowest unfilled electronic orbital corresponds to the t_{1u} representation of the icosahedral symmetry group I_h and that the optical transitions between them are dipole-forbidden. The molecular electronic levels in the C_{60} crystal transform into energy bands, and the lowering of the symmetry of the crystal leads to removal of the degeneracy and to splitting of the levels. The calculations of the equation of state and the band structure of the C_{60} crystal, performed from first principles by the method of the local charge-density functional, by different groups of authors give approximately the same results.^{13,31-33} The bulk modulus calculated in Refs. 32 and 14 is 17.5 and 18.3 GPa, respectively, and it is close to the experimental value 18.1 ± 1.8 GPa.⁴ All calculations of the band structure predict that C_{60} is a semiconductor with a direct gap at the X-point of the Brillouin zone. Different gap widths have been obtained in different calculations: 1.2 eV,³³ 1.34 eV,¹³ and 1.5 eV (Ref. 31). The calculations performed in Refs. 13 and 14 are most convenient for comparing with experimental data. In Refs. 13 and 14 the spectral dependence of the imaginary part of the permittivity, reflecting directly the optical-absorption spectrum, as well as calculations of the band structure for different values of the period of the cubic lattice of the C_{60} crystal are presented. In these calculations the position of the fundamental absorption edge, corresponding to the lowest allowed direct transition between the valence band and the conduction band, was determined. Its value at normal pressure is 1.45 eV and is somewhat greater than the direct gap, which is equal to 1.35 eV and determines the minimum distance between the top of the valence band and the bottom of the conduction band at the X-point of the Brillouin zone.¹⁴

The pressure dependence, determined in Ref. 14, of the band gap and the position of the fundamental absorption edge can be compared to the experimental results on optical absorption and luminescence at high pressure. In Fig. 6 the experimental dependence of the long-wavelength edge of the absorption spectrum (filled squares) and of the short-wavelength edge of the luminescence spectrum (filled circles) as a function of the relative change in the volume V/V_0 of the crystal is presented on a logarithmic scale. The quantity V/V_0 was calculated from the equation of state of the C_{60} crystal

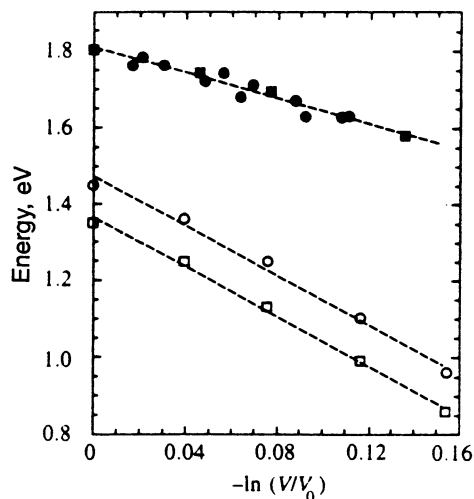


FIG. 6. Experimental dependence of the long-wavelength absorption edge (filled dots) and short-wavelength edge of the luminescence spectrum (filled triangles) as a function of the relative volume V/V_0 , computed position of the absorption edge (open dots) and the band gap (open squares) according to the data of Ref. 14. Dashed straight lines—linear approximation.

$$P = (B_0/B'_0)\{(V_0/V)^{B'_0} - 1\}, \quad (2)$$

where the quantities $B_0 = 18.1 \pm 1.8$ GPa and $B'_0 = dB_0/dP = 5.7 \pm 0.6$, were determined from x-ray measurements on the structure of the C_{60} crystal at high pressure.⁴ The open circles and squares in Fig. 6 represent the computed position of the fundamental absorption edge and the magnitude of the direct gap, respectively.¹⁴ The dashed straight lines are a linear fit to these data, and the slope of the straight lines determines the deformation potential in accordance with the formula

$$D = \frac{\partial E_g}{\partial \ln(V_0/V)} = -B'_0 \frac{dE_g}{dP}. \quad (3)$$

The deformation potential computed from the data of Ref. 14 is equal to approximately 2.5 eV. The experimental value of the deformation potential, determined in the present work from the pressure shift of the long-wavelength edge of the absorption spectrum and the short-wavelength edge of the luminescence spectrum, is equal to 1.3 ± 0.1 eV. It should be noted that the value obtained differs from both the value computed in Ref. 14 and from the values determined previously from the edge transmission and luminescence spectra.^{8,9} At the same time, the value obtained in the present work for the deformation potential is close to the value 1 eV obtained previously in measurements of the pressure dependence of the absorption spectra of thin films of C_{60} .⁷ These differences pertain equally to the magnitude of the pressure shift of the absorption and luminescence spectra of the C_{60} crystal related to the deformation potential by (3). The scatter in the experimental data is associated, in our opinion, with the difference in the accuracy with which the fundamental absorption edge is determined for thin and thick samples. It should be noted that all measurements give close values for the position of the fundamental absorption edge in the range

1.75–1.8 eV. These values are much higher than the theoretical value of 1.45 eV. The authors of the calculations performed by the density-functional method attribute this difference to the overestimation of the gap in this method.¹⁴ Our data on the pressure shift of the absorption and luminescence spectra as well as the magnitude of the deformation potential indicate that the calculations of Ref. 14 also overestimate these values.

In summary, the main results of this work are as follows. The absorption, luminescence, and Raman-scattering spectra of C₆₀ single crystals at high pressure were measured. Features were discovered in the pressure dependence of the Raman-scattering spectra at pressures of 0.4 and 2.4 GPa. These features are associated with the orientational-ordering phase transitions of C₆₀ molecules in the cubic lattice of fullerite. The pressure shifts of the intramolecular phonon modes, the long-wavelength edge of the absorption spectrum, and the short-wavelength edge of the luminescence spectrum were determined. The Grüneisen parameters of the phonon modes in the orientationally ordered phase and the magnitude of the deformation potential were determined. The experimental data obtained were compared with the results of theoretical calculations.

In conclusion, we thank I. N. Kremenskaya for kindly providing the C₆₀ material and V. K. Dolganov for helpful discussions. We thank the Secretary of Scientific Research and Development, Greece, for financial support. K. P. Meletov thanks the Aristotle University in Saloniki, Greece, for hospitality and NATO for financial support.

¹W. Kratschmer, K. Fostiropoulos, and D. Huffman, *Chem. Phys. Lett.* **170**, 167 (1990).

²S. J. Woo, Seubg Hee Lee, Eunja Kim *et al.*, *Phys. Lett. A* **162**, 501 (1992).

³J. E. Fischer, P. A. Heiney, A. R. McGhie *et al.*, *Science* **252**, 1288 (1991).

⁴S. J. Duclos, K. Brister, R. C. Haddon *et al.*, *Nature* **351**, 380 (1991).

⁵D. W. Snoke, Y. S. Raptis, and K. Syassen, *Phys. Rev. B* **45**, 14419 (1992).

⁶K. P. Meletov, V. K. Dolganov, O. V. Zharikov *et al.*, *J. Phys. I France* **2**, 2097 (1992).

⁷F. Moshary, N. Chen, I. Silvera *et al.*, *Phys. Rev. Lett.* **69**, 466 (1992).

⁸A. K. Sood, N. Chandrabhas, D. Victor *et al.*, *Solid State Commun.* **81**, 89 (1992).

⁹D. W. Snoke, K. Syassen, and A. Mittelbach, *Phys. Rev. B* **47**, 4146 (1993).

¹⁰M. Nunez Regueiro, L. Abello, G. Lucazeau *et al.*, *Phys. Rev. B* **46**, 9903 (1992).

¹¹N. Chandrabhas, M. N. Shashikala, D. V. S. Muthy *et al.*, *Chem. Phys. Lett.* **197**, 319 (1992).

¹²K. Meletov, D. Christofilos, G. Kourouklis, and S. Ves, accepted in *Chem. Phys. Lett.* (1995).

¹³W. Y. Ching, Ming-Zhu Huang, Young-Nian Xu *et al.*, *Phys. Rev. Lett.* **67**, 2045 (1991).

¹⁴Ming-Nian, Ming-Zhu Huang, and W. Y. Ching, *Phys. Rev. B* **46**, 4241 (1992).

¹⁵Jin Yu, Lingsing Bi, R. K. Kalia *et al.*, *Phys. Rev. B* **49**, 5008 (1994).

¹⁶A. Jayaraman, *Rev. Sci. Instrum.* **57**, 1013 (1986).

¹⁷D. Barnett, S. Block, and G. J. Piermarini, *Rev. Sci. Instrum.* **44**, 1 (1973).

¹⁸G. Dresselhaus, M. S. Dresselhaus, and P. C. Eklund, *Phys. Rev. B* **45**, 6923 (1992).

¹⁹P. H. M. van Loosdrecht, P. J. M. van Bentum, M. A. Verheijen *et al.*, *Chem. Phys. Lett.* **198**, 587 (1992).

²⁰P. H. M. van Loosdrecht, P. J. M. van Bentum, and G. Meijer, *Phys. Rev. Lett.* **68**, 1176 (1992).

²¹D. S. Bethune, G. Meijer, W. C. Tang *et al.*, *Chem. Phys. Lett.* **179**, 181 (1991).

²²P. A. Heiney, J. E. Fisher, A. R. McGhie *et al.*, *Phys. Rev. Lett.* **66**, 2911 (1991).

²³G. A. Samara, J. E. Schirber, B. Morosin *et al.*, *Phys. Rev. Lett.* **67**, 3136 (1991).

²⁴W. I. F. David, R. M. Ibersen, T. J. S. Dennis *et al.*, *Europhys. Lett.* **18**, 219 (1992).

²⁵A. P. Jephcoat, J. A. Hriljac, L. W. Finger *et al.*, *Europhys. Lett.* **25**, 429 (1994).

²⁶Y. Huang, D. F. R. Gilson, and I. Butler, *J. Phys. Chem.* **95**, 5723 (1991).

²⁷H. Yamawaki, M. Yoshida, Y. Kakudate *et al.*, *J. Phys. Chem.* **97**, 11161 (1993).

²⁸A. M. Rao, Ping Zhou, Kai-an Wang *et al.*, *Science* **259**, 955 (1993).

²⁹C. Reber, L. Yee, J. McKierman *et al.*, *J. Phys. Chem.* **95**, 2127 (1991).

³⁰R. C. Haddon, L. E. Brus, and K. Raghavachari, *Chem. Phys. Lett.* **125**, 459 (1986).

³¹S. Saito and A. Oshiyama, *Phys. Rev. Lett.* **66**, 2637 (1991).

³²N. Troullier and J. L. Martins, *Phys. Rev. B* **46**, 1754 (1992).

³³S. C. Erwin in *Buckminsterfullerenes*, edited by W. E. Billups and M. A. Ciufolini, VCH Publishers, New York, 1992.

Translated by M. E. Alferieff